Maintenance of polygenic local adaptation and reproductive isolation in diploid and haplodiplontic populations

Arthur Zwaenepoel, Himani Sachdeva, Christelle Fraïsse

Abstract

Lorem ipsum dolor sit amet, consectetuer adipiscing elit. Ut purus elit, vestibulum ut, placerat ac, adipiscing vitae, felis. Curabitur dictum gravida mauris. Nam arcu libero, nonummy eget, consectetuer id, vulputate a, magna. Donec vehicula augue eu neque. Pellentesque habitant morbi tristique senectus et netus et malesuada fames ac turpis egestas. Mauris ut leo. Cras viverra metus rhoncus sem. Nulla et lectus vestibulum urna fringilla ultrices. Phasellus eu tellus sit amet tortor gravida placerat. Integer sapien est, iaculis in, pretium quis, viverra ac, nunc. Praesent eget sem vel leo ultrices bibendum. Aenean faucibus. Morbi dolor nulla, malesuada eu, pulvinar at, mollis ac, nulla. Curabitur auctor semper nulla. Donec varius orci eget risus. Duis nibh mi, congue eu, accumsan eleifend, sagittis quis, diam. Duis eget orci sit amet orci dignissim rutrum.

1 Introduction

When a population is subdivided across multiple habitats with different environmental conditions, the extent to which distinct subpopulations can maintain locally beneficial genetic variants depends on the rate of migration between these subpopulations. Migration between populations that maintain divergently selected alleles can lead to maladaptive gene flow, yielding a migration load (a reduction in mean fitness due to the influx of locally maladaptive genes) or may lead to loss of local adaptation altogether (so-called *swamping* by gene flow). While local adaptation may be due to a few conspicuous loci (e.g. industrial melanism in *Biston*; Hof et al. (2016)), it is believed to typically be polygenic, with alleles of different effects responding to selection in the local environment at many loci spread across the genome (Bomblies and Peichel 2022; Stankowski et al. 2022; Westram et al. 2018). When local adaptation is polygenic, migration from a population adapted to different environmental conditions will lead to linkage disequilibria (LD) among selected alleles (i.e. migrant alleles will tend to be found together in the genome), and the rate at which the invading locally deleterious alleles are eliminated by selection will be affected by such associations (Feder, Egan, and Nosil 2012; Yeaman 2015; Sachdeva 2022). This in turn will affect the equilibrium migration load and swamping thresholds for the loci under selection. Neutral variation may also come to be associated with locally selected alleles, so that the latter constitute a 'barrier' to neutral gene flow, increasing neutral genetic differentiation (as quantified by F_{ST} for instance) beyond the single locus neutral expectation. Such barrier effects due to divergent local adaptation may play an important role in the evolution of reproductive isolation, and hence speciation (Nosil 2012).

Despite mounting evidence that local adaptation is often polygenic in nature, little is known about the underlying genetic details: How many loci are involved? What are the typical effect sizes? Are locally beneficial alleles typically closely linked (forming so-called 'genomic islands'), or are they spread all over the genome? How non-additive is local adaptation? *etc.* (e.g. Yeaman 2015; Bomblies and Peichel 2022). Moreover, even assuming such details to be known, it is unclear to what extent the genetic architecture of local adaptation affects the ability of a population to maintain reproductive isolation in the face of gene flow. Conversely, it remains unclear just to what extent one could hope to infer the detailed genetic architecture underlying local adaptation from observed patterns of genomic differentiation, as for instance obtained through so-called 'genome scans'. So far, most theoretical developments have assumed rather simple genetic architectures, dealing with biallelic loci of equal additive effect (ignoring dominance and epistasis) that are either unlinked or uniformly spread along a block of genome; and statistical approaches for the inference of gene flow across the genome either make similarly crude assumptions (Aeschbacher et al. 2017), or ignore the genetic details of local adaptation altogether (Fraïsse et al. 2021; Laetsch et al. 2022).

In a recent paper, Sachdeva (2022) showed that, when the loci under selection are unlinked, the effects of LD on migration-selection balance at any individual locus in a multilocus barrier can be well described by classical (deterministic or stochastic) single locus population genetic theory, provided that the migration rate m is substituted by a suitably defined (selective) *effective* migration rate m_e (Petry 1983; Bengtsson 1985; Kobayashi, Hammerstein, and Telschow 2008), which captures the effects of selection against the associated genetic background. The extent to which *neutral* gene flow is reduced by LD with alleles under selection can be similarly quantified by the (neutral) effective migration rate (Petry 1983; Nicholas H. Barton and Bengtsson 1986; Kobayashi, Hammerstein, and Telschow 2008), which can serve as a quantitative measure of reproductive isolation (Westram et al. 2022). In her paper, Sachdeva (2022) conducted a detailed study of the effects of both drift and LD on swamping thresholds and neutral differentiation in the mailand-island and infinite-island models of population subdivision, assuming a haploid sexual life cycle and L divergently selected loci of equal effect. Here we extend some of this work to investigate the effects of dominance and variation among selective effects on the maintenance of polygenic local adaptation and reproductive isolation in populations with a diploid or haplodiplontic life cycle, focusing on the mainland-island model.

All sexual organisms have a life cycle with a distinct haploid and diploid stage, with remarkable diversity in the relative duration and development of the two phases. The existence of a diploid phase entails that interactions between different alleles at a locus (genetic dominance) will generally affect phenotypic traits and hence fitness. The effects of dominance on equilibrium frequencies and swamping thresholds in the single locus mainland-island model are well known (Haldane 1930; Nagylaki 1975). Consider a diploid model (i.e. a model with no selection in the haploid phase), where the relative fitnesses of genotypes $A_0A_0 : A_0A_1 : A_1A_1$ are given by $1 : 1 - hs : 1 - s$ and where we assume a proportion m of the population is replaced by migrants of the A_1A_1 genotype each generation. For the case $h = 0.5$ (no dominance, also referred to as codominance, or additivity), the equilibrium frequency $\tilde{p}$ of the locally beneficial A_0 allele decreases linearly from 1 to 0 as the rate of migration approaches the strength of selection on a single allele $\frac{s}{2}$. When local adaptation is due to a dominant allele (so that the

invading allele acts recessively to reduce fitness on the island, i.e. $h = 0$), the migration rate beyond which no polymorphism can be maintained is increased to s, while $\tilde{p}$ is decreased relative to the additive case as long as $m < s/4$. When local adaptation is due to a recessive allele ($h = 1$), the model has two equilibria for the beneficial allele frequency, one stable equilibrium $\tilde{p}_+ > 1/2$ and one unstable equilibrium $\tilde{p}_- < 1/2$. The two equilibria collide at the critical migration threshold of $m_c = s/4$, beyond which swamping occurs for any initial frequency. Hence, for the recessive case, whether or not a polymorphism is attained depends not only on the migration rate (which should be at most $s/4$), but also on the history of the population: the island population cannot fix a new recessive beneficial variant, but an established recessive variant can be maintained upon secondary contact. All these phenomena were first noted by Haldane (1930). A main goal of the present paper is to understand how this behavior is affected when we consider the polygenic case.

A second question we aim to address is to what extent LD among alleles with different fitness and dominance effects protects weakly selected alleles in the barrier from swamping and determines variation in the levels of differentiation maintained across the barrier at equilibrium. Despite the many recent large-scale genomic studies, the genetic architecture of local adaptation has remained rather elusive, and it appears relevant to ask, for a given genetic architecture of local adaptation, what sort of signals one is likely to observe in empirical data, and to what extent selective interference between different loci blurs the signatures of individual loci. (linkage to a barrier locus? connect to Yeaman 2015?)

We start by outlining a single locus mainland-island model for a haplodiplontic life cycle which in the weak selection continuous-time limit encompasses both the haplontic, diplontic and haplodiplontic cases. We then extend this to the multilocus setting by deriving an approximation to the effective migration rate based on the expected reproductive value of a migrant individual in the island population. We study the thresholds for swamping in the deterministic multilocus model with L divergently selected loci harboring alleles of equal effect, and find that the effect of increasing the total strength of selection against migrants (Ls) on swamping thresholds and equilibrium differentiation depends rather strongly on the dominance coefficient. We then study the effects of drift on the level of differentiation maintained at equilibrium and consider heterogeneous barrier architectures, where both dominance and the intensity of selection varies across the loci under selection. Throughout, we highlight the remarkable accuracy of the heuristic approach first outlined in Sachdeva (2022), and illustrate how it extends in a rather straightforward way to multilocus models with dominance, haploid selection and heterogeneous selective effects.

2 Model and Methods

2.1 Haplodiplontic mainland-island model

Here we outline a mainland-island model for a sexual population which may be subject to selection in both the haploid and diploid phases. We think of this model as a caricature of a bryophyte, pteridophyte or fungal population, but as we shall see below, the model encompasses both diplontic and haplontic life cycles as well. Throughout, we shall assume that sexes need not be distinguished, and that selfing is possible. We assume a regular and synchronous alternation of generations, where an island population of N haploids (gametophytes) produces

an effectively infinite pool of gametes which unite randomly to form Nk diploid individuals (sporophytes). The Nk diploids produce in turn an effectively infinite pool of haploid spores through meiosis, of which N are drawn to form the next haploid generation. In each generation, we assume M haploid individuals on the island are replaced by haploid individuals from a mainland population, where M is Poisson distributed with mean Nm. The mainland population is assumed to have a constant, but arbitrary, genetic composition. Unless stated otherwise, we shall assume the mainland to be fixed for the locally deleterious allele on the island. Fitness on the island is determined by L unlinked biallelic loci which are under divergent selection relative to the mainland. Fitness effects are allowed to vary arbitrarily across loci. Denoting the alleles at locus i by $A_{i,0}$ and $A_{i,1}$, we designate by $w_{i,j}$ the relative fitness of the haploid genotype $A_{i,j}$ and $w_{i,jk}$ the relative fitness of diploid genotype $A_{i,j}A_{i,k}$. We suppress the index i when considering a generic locus. We assume throughout that $w_0 = 1$ and $w_1 = e^{s_1}$ for the haploid phase, and $w_{00} = 1, w_{01} = w_{10} = e^{s_{01}}$, and $w_{11} = e^{s_{11}}$ for the diploid phase. Throughout, we denote the frequency of the allele with relative fitness 1 at locus i by p_i, and the frequency of the alternative allele by $q_i = 1 - p_i$. Fitness is determined multiplicatively across loci, so that, for instance, the log relative fitness of a haploid individual fixed for all the '1' alleles (genotype $A_{1,1}, A_{2,1}, \ldots, A_{L,1}$) is given by $\log w = \sum_{i=1}^{L} s_{i,1}$. We assume that each haploid (diploid) individual contributes gametes (spores) to the gamete (spore) pool proportional to its fitness. We assume symmetric mutation at a small constant rate u per locus, occurring at meiosis.

Individual-based simulations of this model are implemented in Julia (Bezanson et al. 2017) and the code is available at GitHub. In the following sections, we build up a theoretical approximation to this fairly general multilocus model, roughly as in Sachdeva (2022). We first derive the dynamics at a single locus, considering both deterministic and stochastic models. Next, we derive an approximation to the effective migration rate in the multilocus system using a rather general argument based on the reproductive value of migrant individuals. Lastly, we approximate the allele frequency dynamics of the multilocus model by plugging in the effective migration rate, which captures the effect of LD among selected alleles on the dynamics at a neutral locus, in the single locus theory.

2.2 Single locus mainland-island model

2.2.1 Deterministic dynamics

We first consider a deterministic model for the allele frequency dynamics at a single focal locus, ignoring the influence of the other loci as well as genetic drift. As shown in detail in sec. S2.1, for weak selection and migration, the dynamics of p can be described in continuous time by the nonlinear ordinary differential equation (ODE)

$$\dot{p} := \frac{dp}{dt} = -m(p - p_M) - q(s_a p + s_b pq) \ , \tag{1}$$

where $s_a = s_1 + s_{01}$ and $s_b = s_{11} - 2s_{01}$, the latter being a measure of dominance (i.e. the deviation from multiplicative fitnesses, sometimes called ι (Otto 2003; Manna, Martin, and Lenormand 2011)). Usually, s_1, s_{01} and s_{11} will be assumed to be negative, and p_M will be assumed to be small, so that selection increases p, whereas migration decreases p. As expected, this is the same dynamical law as for a strictly diploid model, in which case $s_a = s_{01}$. This

enables us to identify a pair of selection coefficients $s^*_{01} = s_1 + s_{01}$ and $s^*_{11} = 2s_1 + s_{11}$. When $s^*_{11} \neq 0$, we can hence describe the haplodiplontic system as the familiar diploid model with some effective degree of dominance $h_e = s^*_{01}/s^*_{11} = \frac{s_1+s_{01}}{2s_1+s_{11}}$ and an effective selection coefficient $s_e = s^*_{11} = 2s_1 + s_{11}$, at least when selection is sufficiently weak so that allele frequencies do not change appreciably within any one alternation of generations. The equilibria of eq. 1 are analyzed in detail in sec. S2.2.

2.2.2 Diffusion approximation to the stochastic dynamics

Still considering a single focal locus, we now account for the effects of sampling drift. Denoting by X_n the number of A_1 copies in the nth haploid generation, and by $Y_n^{(ij)}$ the number of A_iA_j genotypes in the nth diploid generation, the life cycle as outlined in sec. 2.1 entails the following Markov chain model:

$$Y_n|X_n \sim \mathrm{HW}\left(Nk, \frac{w_{h,1}}{\bar{w}_h}\frac{X_n}{N}\right) \tag{2}$$

$$X_{n+1}|Y_n \sim \mathrm{Bin}\left(N, \frac{\bar{w}_{d,1}}{\bar{w}_d}\left(\frac{Y_n^{(11)} + Y_n^{(01)}/2}{Nk}\right)\right) , \tag{3}$$

where $w_{h,1}$ ($\bar{w}_h$) and $\bar{w}_{d,1}$ ($\bar{w}_d$) are the marginal fitnesses of the A_1 allele (mean fitnesses) in the haploid and diploid generation respectively, and where $\mathrm{HW}(N, p)$ refers to the multinomial distribution with Hardy-Weinberg proportions at allele frequency p for population size N. Note that one unit of time corresponds to a single *alternation* of generations, involving two sampling stages: first we sample diploid genotypes from the random union of fitness-weighted haploid genotypes (eq. 2), next we sample haploid spores by randomly drawing gene copies from the diploid genotypes that survive diploid selection (eq. 3). This Markov chain model is readily extended to include mutation and migration. This model is akin to the standard Wright-Fisher (WF) model for a diploid or haploid population. Indeed, for the neutral case, it is easily seen that the model corresponds to a haploid WF model with variable population size, regularly alternating between N and $2Nk$ gene copies. The corresponding effective population size is hence $N_e = (N^{-1} + (2Nk)^{-1})^{-1}$, twice the harmonic mean of the phase-specific number of gene copies (Hein, Schierup, and Wiuf 2004) (twice because our unit of time is an alternation of generations, not a single generation).

When evolutionary forces are sufficiently weak, diffusion theory can be applied to approximate the equilibrium allele frequency distribution implied by the above Markov chain by a continuous density $\phi(p)$ on the unit interval. Specifically, we have (e.g. Felsenstein 2005; Ewens 2004):

$$\phi(p) \propto V(p)^{-1} \exp\left[2\int_0^p \frac{M(x)}{V(x)}dx\right],$$

where for the haplodiplontic mainland-island model, the infinitesimal mean and variance will be, respectively,

$$M(p) = -q(s_a p + s_b pq) + u(q - p) - m(p - p_M)$$
$$V(p) = N_e^{-1} pq \ .$$

This yields a probability density function for the equilibrium allele frequency distribution

$$\phi(p; N_e, u, m, s) \propto p^{2N_e(u+mp_M)-1} q^{2N_e(u+mq_M)-1} e^{N_e(2s_a q + s_b q^2)}, \tag{4}$$

where no closed form expression is known for the normalizing constant. This is essentially Wright's (Wright 1937) distribution for a general haplodiplontic life cycle.

2.3 Multilocus model

2.3.1 Effective migration rate

To begin constructing a useful approximation to the allele frequency dynamics in the multilocus system, we derive an appropriate expression for the effective migration rate m_e, which captures the reduction in gene flow at a focal locus due to selection against migrant genotypes. As shown formally in Kobayashi, Hammerstein, and Telschow (2008), for weak migration, the reduction in gene flow relative to the 'raw' migration rate m, termed the *gene flow factor* (gff), depends on the expected reproductive value of migrants in the resident background. At any time, the proportion of individuals with recent migrant ancestry on the island is $O(m)$, so that the probability of individuals with migrant backgrounds mating with each other to produce, for instance, F2 crosses of the migrant and resident genotypes, is $O(m^2)$, and hence negligable for sufficiently weak migration. Let $W_{h,k}$ and $W_{d,k}$ denote the relative fitness of an individual derived from a kth generation haploid, respectively diploid, backcross of an initial migrant individual with the resident population (i.e. $W_{d,1}$ is the relative fitness of an F1 diploid, $W_{d,2}$ of an offspring from a F1 × resident cross (BC1 generation), *etc.*). Assuming migration occurs in the haploid phase before selection, the gff can be expressed as

$$g = \frac{m_e}{m} = \mathbb{E}[W_{h,0} \prod_{k=1}^{\infty} W_{d,k} W_{h,k}], \tag{5}$$

where $W_{h,0}$ is the relative fitness of the haploid migrant in the resident population (Westram et al. 2018; Nicholas H. Barton and Etheridge 2018; Sachdeva 2022). Note that this involves an expectation over all possible lines of descent of an initial migrant spore. In order to derive a useful approximate expression for g, we shall make two further important assumptions: (1) both the resident and migrant gene pools are are in Hardy-Weinberg and linkage equilibrium; (2) variation and selection among offspring of a kth generation migrant descendant × resident cross (i.e. segregation variance within F1s, BC1s, *etc.* and selection thereupon) is negligable. This last assumption becomes more plausible as local adaptation is due to more and more loci of smaller effect.

Under these assumptions, each of the $W_{\cdot,k}$ is determined solely by the frequencies of the selected alleles in the mainland and the island populations at the assumed equilibrium. This allows us to determine $\mathbb{E}[q_{i,k}]$, the expected frequency of the locally deleterious allele at locus i among kth generation descendants from a migrant, in terms of the allele frequencies in the mainland and island population. Indeed, assumption (3) implies the recursive relation $q_{i,k} = \frac{1}{2}(q_{i,k-1} + q_i)$, where q_i is the allele frequency in the resident population – i.e. the average number of selected alleles carried by a kth generation backcross is the mean of the number of such alleles carried by a $k-1$th generation backcross and a resident individual. Hence, we have $\mathbb{E}[q_{i,k}] = \frac{1}{2^k}(q_{M,i} + (2^k - 1)\mathbb{E}[q_i])$, where $q_{M,i} = q_{0,i}$ is the mainland frequency.

Denoting the selection coefficient at locus i for the haploid phase by s_{i1}, we can use this to derive the expected relative fitness of a kth generation haploid descendant:

$$\begin{aligned}\mathbb{E}[W_{h,k}] &= \mathbb{E}\left[\frac{\prod_{i=1}^{L}(p_{k,i}+q_{k,i}e^{s_{i1}})}{\prod_{i=1}^{L}(p_i+q_ie^{s_{i1}})}\right] \\ &= \frac{\prod_{i=1}^{L}\mathbb{E}\left[1-q_{k,i}(1-e^{s_{i1}})\right]}{\prod_{i=1}^{L}\mathbb{E}\left[1-q_i(1-e^{s_{i1}})\right]} \\ &\approx \exp\left[\sum_{i=1}^{L}s_{i1}\mathbb{E}[q_{k,i}-q_i]\right] \\ &= \exp\left[2^{-k}\sum_{i=1}^{L}s_{i1}(q_{M,i}-\mathbb{E}[q_i])\right]\end{aligned}$$

where we have assumed that per-locus selection is sufficiently weak so that terms which are $O(s^2)$ can be ignored. For the diploid phase, a similar argument shows that for the $(k+1)$th generation,

$$\mathbb{E}[W_{d,k+1}] = \exp\left[2^{-k}\sum_{i=1}^{L}s_{i01}(q_{M,i}-\mathbb{E}[q_i]) - s_{i,b}(p_{M,i}\mathbb{E}[q_i]-\mathbb{E}[p_iq_i])\right],$$

where s_{i01} and s_{i11} are the selection coefficients against heterozygotes and homozygotes at locus i respectively, and where, analogous to the single locus model, $s_{i,b} = s_{i11} - 2s_{i01}$. Putting everything together, the approximate gff becomes

$$\begin{aligned}g &\approx \mathbb{E}[W_{h,0}]\prod_{k=1}^{\infty}\left(\mathbb{E}[W_{d,k}]\mathbb{E}[W_{h,k}]\right) \\ &= \prod_{k=0}^{\infty}\exp\left[2^{-k}\sum_{i=1}^{L}s_{i,a}(q_{M,i}-\mathbb{E}[q_i]) - s_{i,b}(p_{M,i}\mathbb{E}[q_i]-\mathbb{E}[p_iq_i])\right] \\ &= \exp\left[2\sum_{i=1}^{L}s_{i,a}(q_{M,i}-\mathbb{E}[q_i]) - s_{i,b}(p_{M,i}\mathbb{E}[q_i]-\mathbb{E}[p_iq_i])\right] \qquad (6)\end{aligned}$$

where, similarly, $s_{i,a} = s_{i1} + s_{i01}$. It is worth stressing that the gff is a function of the actual differentiation between the mainland and island population, and that although we assume migration is sufficiently rare, we do *not* assume that alleles of the type introduced by migrants are rare. We shall often highlight the dependence of the gff on the allele frequencies by writing $g[p]$. If we assume all loci to have the same selection coefficients, and that the mainland is fixed for the locally deleterious allele on the island, the gff simplifies to

$$g = e^{2L(s_a\mathbb{E}[p]+s_b\mathbb{E}[pq])} \qquad (7)$$

where $\mathbb{E}[p]$ and $\mathbb{E}[pq]$ are the expected beneficial allele frequency and expected heterozygosity at any selected locus on the island. Note that in our applications $s_a < 0$, so that when the locally beneficial allele is common ($p \approx 1$) and Ls_a is appreciable, gene flow will indeed be reduced due to selection against migrants.

To gain some intuition for this result, we can express eq. 8 in terms of the effective selection coefficient s_e against the invading allele, and the effective dominance coefficient h_e of the invading allele over the locally beneficial one, as

$$g = e^{-2Ls_e h_e \mathbb{E}[p]} e^{-2Ls_e(1-2h_e)\mathbb{E}[pq]} \tag{8}$$

(see sec. 2.2.1). Here, the first factor is just the gff associated with a haploid L-locus system with selection coefficients $s_e h_e$ (Sachdeva 2022). The second factor captures the effects of dominance when heterozygosity is appreciable. Clearly, h_e has opposing effects on both factors. The immediate effect of dominance is therefore that the gff is decreased (barrier strength increased) relative to the additive case whenever invading alleles exhibit a dominant deleterious effect on the island ($h_e > 1/2$). Only when heterozygosity ($\mathbb{E}[pq]$) becomes appreciable does the second factor contribute to the increase (when $h_e > 1/2$) or decrease (when $h_e < 1/2$) of the gff. The implications of these observations for the maintenance of adaptive differentiation will be explored in detail in the results section.

Two remarks are due. Firstly, the gff as derived above yields the effective migration rate at an unlinked neutral locus. If we wish to calculate the effective migration rate for a selected locus in the barrier, say locus j, the relevant gff is

$$g_j = \exp\left[2\sum_{i\neq j}^{L} s_{i,a}(q_{M,i} - \mathbb{E}[q_i]) - s_{i,b}(p_{M,i}\mathbb{E}[q_i] - \mathbb{E}[p_i q_i])\right] \tag{9}$$

where we have assumed that the gff at a selected locus is the same as that of a neutral locus at the same location – an assumption which is only expected to work well if selection at the focal locus is sufficiently weak. Secondly, as in the model outlined in sec. 2.1, we have assumed that migration occurs at the start of the haploid phase, reflecting a process such as spore dispersal in bryophytes, pteridophytes or Fungi. However, it should be emphasized that, while the details of when migration occurs in the life cycle do not matter for the single locus model as long as selection and migration are sufficiently weak (so that the continuous-time limit is appropriate), these details *do* matter for the effective migration rate. This is because, although selection *per locus* is weak (s being small), selection against migrant genotypes can be strong (Ls being appreciable). Two other cases should hence be considered. Firstly, when migration is due to dispersal of gametes, the first generation experiencing selection on the island will be the diploid F1 generation, so that the appropriate gff under the same approximation is $g/\mathbb{E}[W_{h,0}]$. Secondly, when migration occurs at the beginning of the diploid phase (e.g. seed dispersal), the first generation experiencing selection on the island will consist of diploid migrant individuals, so that $g\mathbb{E}[W_{d,0}]$ is the appropriate gff, where

$$\mathbb{E}[W_{d,0}] = \exp\left[\sum_{i=1}^{L} s_{i11}(q_M - \mathbb{E}[q]) + s_{b,i}(\mathbb{E}[pq] - p_M q_M)\right]$$

In the present work, we shall always assume migration is due to dispersal of haploid spores, so that eq. 6 gives the relevant gff.

2.3.2 Dynamics and equilibria for the multilocus model

The gff captures the effect of LD among selected loci on the rate of gene flow from the mainland into the island at any individual locus. The key observation is that a certain separation of

time scales applies: although selection against migrant *genotypes* can be very strong in the polygenic case (of magnitude Ls, roughly), selection at any individual locus is still assumed to be weak, so that after an evolutionarily short period in which entire sets of alleles are efficiently removed together, LD among selected loci quickly becomes negligable and the standard single locus theory should be appliccable. Hence, on the longer time scales at which migration-selection balance is attained, the allele frequency dynamics at any individual locus should essentially follow the single locus dynamics, but where migrant alleles are introduced at a reduced rate (Sachdeva 2022).

As a consequence, in the deterministic case, we expect that the effects of LD should be well captured by substituting the effective migration rate $m_e = mg$ for m in eq. 1. Specifically, we get a system of L coupled differential equations, where for $1 \leq j \leq L$,

$$\dot{p_j} = -mg_j[p_{-j}]p_j - q_j(s_{a,j}p_j + s_{b,j}p_jq_j) \ , \tag{10}$$

and we have assumed the mainland to be fixed for the deleterious allele on the island at all loci. Here we write $g_j[p_{-j}]$ for the gff as in eq. 9, to highlight the dependence of the gff at locus j on the $L-1$ other loci. We study the equilibria of this model by numerically solving for p at stationarity ($\dot{p_j} = 0$, for $1 \leq j \leq L$).

As in Sachdeva (2022), we can also plug in m_e in the single locus diffusion approximation to determine the equilibrium allele frequency distribution for each locus on the island. Specifically, we postulate that the joint distribution of allele frequencies in the barrier factorizes as

$$\phi(p) = Z^{-1}\prod_{j=1}^{L}\phi_j(p_j|p_{-j}) = Z^{-1}\prod_{j=1}^{L}\phi(p_j; N_e, u, mg_j[p_{-j}], s_j)$$

where Z is a normalizing constant (this can be thought of as a Markov random field over the complete graph with L vertices). We can compute the expected allele frequencies by solving the system self-consistently, assuming $\mathbb{E}[p_j] = Z_j^{-1}\int p_j\phi_j(p_j|\mathbb{E}[p_{-j}])dp_j$. Specifically, assuming the mainland to be fixed for the deleterious allele on the island at all loci, we solve the nonlinear system of $2L$ equations

$$\mathbb{E}[p_j] = Z^{-1}\int p^{2N_eu}q^{2N_e(u+mg_j[\mathbb{E}[p_{-j}]])-1}\psi_j(p)dp$$
$$\mathbb{E}[p_jq_j] = Z^{-1}\int p^{2N_eu}q^{2N_e(u+mg_j[\mathbb{E}[p_{-j}]])}\psi_j(p)dp,$$

where

$$g_j[\mathbb{E}[p_{-j}]] = e^{\sum_{i\neq j}^{L} s_{a,i}\mathbb{E}[q_i]+s_{b,i}\mathbb{E}[p_iq_i]}$$
$$\psi_j(p_j) = e^{N_e(2s_{j,a}q_j+s_{b,j}q_j^2)},$$

for $\mathbb{E}[p_j]$ and $\mathbb{E}[p_jq_j]$. To do so, we use the fixed point iteration outlined in sec. S2.4.

3 Results

3.1 Barrier effect and swamping thresholds in the deterministic model

We first analyze the deterministic multilocus model for a homogeneous barrier, where the fitness and dominance effects of all loci are the same. We shall assume the mainland to be

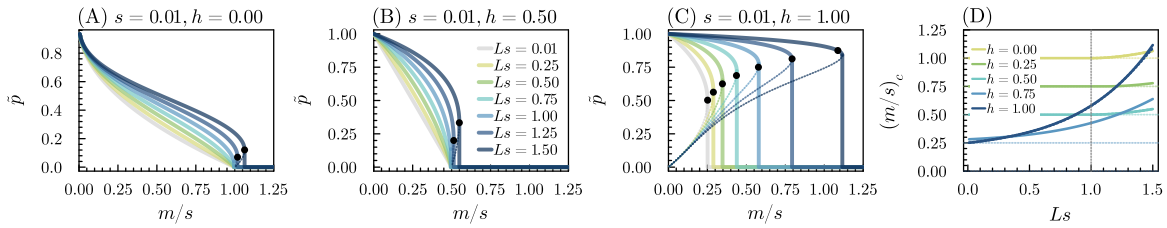

Figure 1: Equilibrium differentiation and swamping thresholds for the deterministic multilocus model. Equilibrium frequencies for increasing Ls are shown for (A) the case of dominant local adaptation (recessive migrant alleles), (B) additive fitness effects and (C) recessive local adaptation. The thick lines show the stable equilibria for increasing m/s, whereas the dotted lines show unstable equilibria. The black dots mark the critical point beyond which swamping is obtained for any initial condition (in (C) the approximate expression discussed in the main text is used). The results for $Ls = 0.01$ (gray lines) correspond to the single locus predictions. (D) Swamping thresholds for different degrees of dominance for increasing total barrier strength Ls.

fixed for the locally deleterious allele at all loci. We only consider diploid selection here, with $s_{01} = -sh$ and $s_{11} = -s$, where s is the selection coefficient against the locally deleterious allele, and $h = s_{01}/s_{11}$ is the dominance coefficient. Note that h measures dominance of the mainland allele over the island allele, so that $h = 1$ corresponds to a situation where the invading allele is fully dominant, or, equivalently, where the allele that confers local adaptation on the island is recessive. For the case where migration is at the haploid stage, restricting the analysis to diploid selection incurs no loss of generality, as haploid selection then simply amounts to a rescaling of the dominance and selection coefficients (see methods). The effective dominance coefficient when there is haploid selection with intensity s_1 will be $h_e = \frac{s_1+s_{01}}{2s_1+s_{11}}$, so that the effect of haploid selection is to pull h_e towards the additive case ($h = 0.5$).

In the homogeneous deterministic model, all loci have the same dynamics if the initial allele frequencies are equal. From eq. 10, we find that in that case, the frequency p of the locally beneficial allele at any individual selected locus in an $L + 1$ locus system must satisfy at equilibrium

$$0 = shpq + s(1-2h)pq^2 - mg[p]p \qquad (11)$$
$$\text{where} \quad g[p] = e^{-2Ls(hp+(1-2h)pq)}.$$

We can solve this numerically for the equilibrium allele frequency. Fig. 1 shows the equilibrium behavior for a number of example parameter sets. As expected, increasing the total strength of selection (Ls) increases the equilibrium frequency of the locally beneficial allele with respect to the single locus prediction, but the magnitude of this effect depends quite strongly on dominance. In particular the effect is much more pronounced when local adaptation is due to recessive variants ($h = 1$). In this case, the gff is at its minimum, and hence the impact of LD on migration-selection balance is strongest, when the deleterious allele is rare (fig. S2). On the other hand, when the invading alleles are recessive ($h = 0$), gene flow is not at all impeded when the deleterious allele is rare (the gff being near one). When $h < 1/3$, the barrier strength, as measured by g^{-1} (Nicholas H. Barton and Bengtsson 1986), *increases* as the deleterious allele increases in frequency on the island, decreasing the rate of gene flow, until a value of $q = (3h-1)/(4h-2)$ is reached (fig. 1, fig. S2). This is essentially because in the latter case,

irrespective of how many deleterious alleles a migrant carries, if the deleterious alleles are rare on the island they will not be found in homozygotes as long as migration is sufficiently weak, and hence will not be 'seen' by selection. On the other hand, when the deleterious alleles are segregating at appreciable frequencies on the island, F1, BC1, *etc.* individuals will be more likely to be homozygous at several loci, thus exposing invading alleles to selection and reducing the RV of migrants. As a result, when invading alleles at the selected loci act recessively, a strong genome-wide barrier effect emerges only once differentiation falls below a critical threshold. The situation is clearly different when migrant alleles are dominant, as the invading alleles will immediately express their full load in the resident population, irrespective of the other allele at the locus, yielding efficient selection against migrant alleles. When the frequency of the deleterious allele increases on the island, this will merely increase the expected relative fitness of migrants in the resident background, and hence reduce the efficiency of selection against migrant genotypes.

Fig. 1 shows that the swamping thresholds are also considerably affected by dominance. For $h = 0$ and $h = 0.5$, the multilocus model starts to exhibit qualitatively different features compared to the single locus model as Ls increases, with bistable behavior and correspondingly sharp thresholds for the loss of local adaptation when Ls is sufficiently large. We now take a closer look at these equilibria and their critical behavior. Clearly, $p = 0$ is always a solution of eq. 11, and it will correspond to a locally stable equilibrium (i.e. swamping) whenever $m/s > 1 - h$. Other equilibria, when they exist, are given by the zeros of the function

$$f(p) = hq + (1 - 2h)q^2 - \frac{m}{s}g[p] \tag{12}$$

Note that $g[p] > 0$ and we assume $s > 0$, so that for any fixed h, as m increases, there will indeed be a critical migration rate beyond which $f(p) < 0$, from which point onwards the only stable equilibrium will be $p = 0$. At the critical point, the equilibrium allele frequency will satisfy the additional constraint $f'(p) = 0$ (see fig. S1)[1],

$$f'(p) = h + 2(1 - 2h)q - 2Lm(1 - 3h - 2(1 - 2h)q)g[p] = 0 \tag{13}$$

We can solve eq. 12 for $g[p]$, and then plug in $g[p]$ in eq. 13. This yields a cubic polynomial in p which can be solved for the allele frequency p_c at the critical point. We can then plug p_c into eq. 12 and solve for m_c/s. While the general expressions yield not much insight, we can focus on a number of special cases.

Firstly, in the additive case ($h = 0.5$), a critical point different from $1 - h$ appears when $Ls > 1$, in which case the equilibrium frequency at the critical point will be $p_c = 1 - 1/Ls$. The corresponding critical migration rate is

$$\frac{m_c}{s} = \frac{e^{Ls-1}}{2Ls}.$$

In the case where local adaptation is due to dominant alleles ($h = 0$), we have again critical behavior as soon as $Ls > 1$, with the swamping threshold occurring at $m/s = 1$ otherwise. In

[1]This appears to hold for arbitrary h, at least I've convinced myself of this using some graphs. Haven't proved that it does though.

this case, we find

$$p_c = \frac{3}{4} - \frac{\sqrt{Ls(Ls+8)}}{4Ls} < \frac{1}{2}, \qquad \frac{m_c}{s} = \left(\frac{1}{4} + \frac{\sqrt{Ls\,(Ls+8)}}{4Ls}\right)^2 e^{\frac{Ls}{4}+\frac{\sqrt{Ls(Ls+8)}}{4}-1}.$$

In contrast with the additive case (where as Ls increases, arbitrary equilibrium differentiation can be maintained near the critical point), equilibrium differentiation will be below 0.5 near m_c when $h = 0$. Lastly, for recessive local adaptation ($h = 1$), we have bistable critical behavior for all $Ls > 0$. The equilibrium frequency at the critical point is always larger than $1/2$ and is given by the zeros of the cubic polynomial

$$4Lsp^3 - 4Lsp^2 + 2p - 1 = 0$$

for which we have no simple expressions. A fair approximation for $Ls < 1.5$ is given by

$$p_c \approx \frac{1}{2} + \frac{Ls}{4}, \qquad \frac{m_c}{s} \approx \left(\frac{1}{4} - \frac{(Ls)^2}{16}\right) e^{\left(\frac{Ls}{2}\right)^3 + \left(\frac{Ls}{\sqrt{2}}\right)^2 + \frac{Ls}{2}}$$

The swamping threshold is seen to increase strongly with increasing Ls. This stuff should move to an appendix, it does not provide much insight beyond the graph (it does clarify that one needs $Ls > 1$ before any change in the critical migration rate is seen, and what sort of differentiation one sees near the critical point). Should figure out for arbitrary h what the Ls is for which one gets critical behavior see also fig. S3.

3.2 Accounting for drift and comparison to individual-based simulations

While the deterministic analysis points towards important effects of dominance on equilibrium differentiation and swamping thresholds, it is important to assess whether we expect such effects to be as pronounced in finite populations. Indeed, Sachdeva (2022) showed that, for small populations, the sharp thresholds for swamping predicted by the deterministic multilocus theory when Ls is appreciable need not apply, and that the critical migration rate may be significantly reduced. Furthermore, it is hard to evaluate the accuracy of our approximations against simulations, as any individual-based simulation will necessarily exhibit genetic drift.

We find that the remarkable accuracy of the heuristic multilocus diffusion approximation observed in Sachdeva (2022) extends to the case with dominance. Indeed, even in parameter regimes where the approximation is expected to break down (Ls appreciable with L small and s large, small population size) we obtain good predictions (fig. S4). Not only can we reliably obtain the expected frequency of alleles on the island, we also obtain very good predictions for the entire allele frequency distribution as observed in individual-based simulations (fig. 2). The bistability observed in the deterministic model, in particular when local adaptation is recessive ($h = 1$), manifests as multimodality in the equilibrium allele frequency distribution. Although the equilibrium allele frequency distribution should be independent of the initial condition (the individual-based model can be thought of as an ergodic Markov chain on the space of N L-locus genotypes), for appreciable Ls, the observed allele frequency distribution in any finite-time simulation can depend strongly on the initial conditions (that is, as Ls increases, stochastic jumps between the different modes of the L-dimensional joint allele

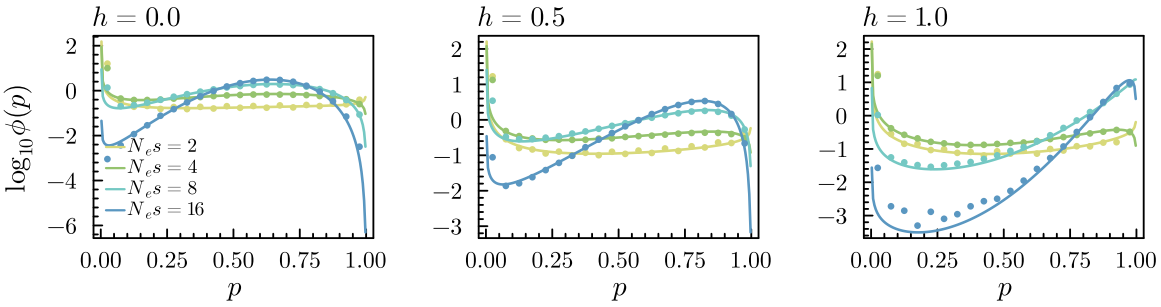

Figure 2: Predicted allele frequency distributions for the diploid multilocus model with homogeneous selective effects for different values of N_e and h (dominance coefficient of the invading alleles). Lines show the numerical approximations based on the diffusion theory, dots show results from individual-based simulations, based on taking a sample every 10 generations for 50000 generations after an initial 10000 generations to reach equilibrium. Other parameter settings are $Ls = 0.8, L = 40, m/s = 0.2, u = 0.005s$.

frequency distribution become increasingly less likely, and occur on time scales that are neither biologically relevant nor computationally feasible). The fixed point iteration will in that case converge to an expectation computed near one of the modes of the allele frequency distribution (see fig. S5 for an illustration). Throughout, we shall assume a scenario of secondary contact, so that the island starts as fixed for the locally beneficial allele at all loci. We note, however, that if different initial conditions are of interest, our simulations suggest that the numerical approach remains accurate. Furthermore, we can use the method to characterize the parameter regime in which the detailed history of the population is likely to matter for the evolution and maintenance of locally beneficial variation.

The general effects of genetic drift are as expected, in that the barrier effect is considerably reduced as N_e decreases (fig. S6). The characteristic effects of dominance hence only become apparent for appreciable N_e. For large population sizes, we now see clearly that for dominant local adaptation (invading alleles are (partially) recessive, $h < 0.5$), two phases can be distinguished as the migration rate increases. As noted above, the barrier strength increases initially as migration increases, so that as long as the deleterious allele is below some frequency determined by h, the equilibrium differentiation declines less fast with increasing m. Once a threshold frequency is reached, the barrier strength declines again as m increases (fig. S6 $h = 0$ and $h = 0.25$ panels). perhaps not worth to spell out.

We now consider in more detail to what extent our approximations apply to the case with both selection in the haploid and diploid phase. In fig. 3, we parameterize the model in such a way that we can investigate, for a given total barrier strength (corresponding to the fitness difference between an island population fixed for the locally beneficial and an island fixed for the locally deleterious allele) the effects of the relative strength of selection in the diploid and the haploid phase and the degree of dominance in the diploid phase. To this end, we assume

$$s_1 = -(1-\tau)s \qquad s_{01} = -h\tau s \qquad s_{11} = -\tau s,$$

where $0 \leq \tau \leq 1$ measures the relative strength of selection in the diploid phase (if one assumes selection to operate continuously with constant intensity throughout the life cycle, this can be interpreted as the relative length of the diploid phase). Similar models have appeared in

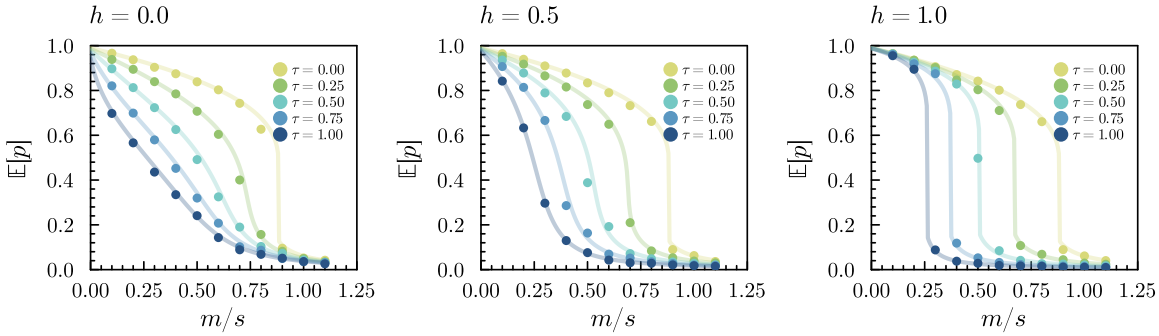

Figure 3: Multilocus migration-selection balance and swamping with dominance and haploid selection. For a given total barrier strength (see main text), we vary the relative strength of selection in the diploid and haploid phase (τ) and the degree of dominance in the diploid phase. Specifically, we assume $s_1 = -(1-\tau)s, s_{01} = -h\tau s$ and $s_{11} = -\tau s$. Other parameters were as follows: $Ls = 0.8, L = 40, N_e s = 8, k = 5, u = s/100$.

the study of life cycle modifiers, see for instance, Otto (1994) and Scott and Rescan (2017). Using this parameterization, we find that when selection is not too strong, we can indeed accurately predict equilibrium frequencies for haplodiplontic life cycles where selection occurs in both the haploid and diploid phase. Furthermore, these results suggest that, for a given total strength of selection, predominantly haploid populations should be able to maintain more adaptive variation, and exhibit stronger reproductive isolation, irrespective of the degree of dominance in the diploid phase. Although haploid selection pulls the effective dominance coefficient towards 0.5 (so that one might expect, based on our results for diploids above, that a diploid phase with recessive local adaptation would enable more adaptive differentiation), the effective selection coefficient in this model is $(2-\tau)s$, so that the strength of selection per gene in haploids is twice that in diploids in the absence of dominance. The relevance of these observations for the evolution and maintenance of haplodiplontic life cycles is however not very clear, as a life cycle modifier need not keep the overall strength of selection constant (Scott and Rescan 2017).

3.3 Heterogeneous genetic architectures

In sec. 2.3, we developed the multilocus theory for potentially heterogenous unlinked architectures, where the s_1, s_{01} and s_{11} can vary arbitrarily across loci. We verify that we obtain accurate predictions also in this setting, using simulations with randomly sampled selection and dominance coefficients (fig. 4).

4 References

Aeschbacher, Simon, Jessica P Selby, John H Willis, and Graham Coop. 2017. "Population-Genomic Inference of the Strength and Timing of Selection Against Gene Flow." *Proceedings of the National Academy of Sciences* 114 (27): 7061–66.

Barton, Nicholas H., and Bengt Olle Bengtsson. 1986. "The Barrier to Genetic Exchange Between Hybridising Populations." *Heredity* 57 (3): 357–76.

Barton, Nicholas H, and AM Etheridge. 2018. "Establishment in a New Habitat by Polygenic

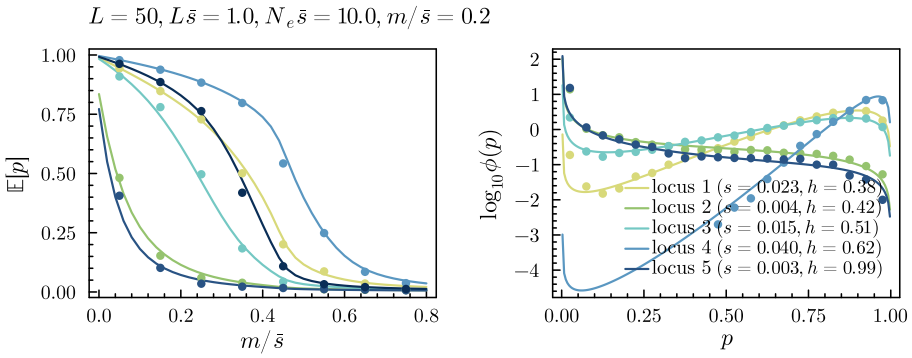

Figure 4: Predicted equilibrium allele frequencies for increasing migration rates (left) and frequency distributions (right) for six loci in a L-locus multilocus barrier in a diploid system, where $s \sim$ Exponential($\bar{s} = 0.02$) and $h \sim$ Beta$(1, 1)$. Lines show predictions from the multilocus diffusion approximation, whereas dots show results from individual-based simulations (simulating for 200000 generations after an initial 10000, sampling every 10th generation).

Adaptation." *Theoretical Population Biology* 122: 110–27.

Bengtsson, BO. 1985. "The Flow of Genes Through a Genetic Barrier." *Evolution: Essays in Honour of John Maynard Smith* 1: 31–42.

Bezanson, Jeff, Alan Edelman, Stefan Karpinski, and Viral B Shah. 2017. "Julia: A Fresh Approach to Numerical Computing." *SIAM Review* 59 (1): 65–98.

Bomblies, Kirsten, and Catherine L Peichel. 2022. "Genetics of Adaptation." *Proceedings of the National Academy of Sciences* 119 (30): e2122152119.

Ewens, Warren John. 2004. *Mathematical Population Genetics: Theoretical Introduction*. Vol. 1. Springer.

Feder, Jeffrey L, Scott P Egan, and Patrik Nosil. 2012. "The Genomics of Speciation-with-Gene-Flow." *Trends in Genetics* 28 (7): 342–50.

Felsenstein, Joseph. 2005. "Theoretical Evolutionary Genetics." *University of Washington, Seattle*.

Fraïsse, Christelle, Iva Popovic, Clément Mazoyer, Bruno Spataro, Stéphane Delmotte, Jonathan Romiguier, Etienne Loire, et al. 2021. "DILS: Demographic Inferences with Linked Selection by Using ABC." *Molecular Ecology Resources* 21 (8): 2629–44.

Haldane, John Burdon Sanderson. 1930. "A Mathematical Theory of Natural and Artificial Selection.(part VI, Isolation.)." In *Mathematical Proceedings of the Cambridge Philosophical Society*, 26:220–30. 2. Cambridge University Press.

Hein, Jotun, Mikkel Schierup, and Carsten Wiuf. 2004. *Gene Genealogies, Variation and Evolution: A Primer in Coalescent Theory*. Oxford University Press, USA.

Hof, Arjen E van't, Pascal Campagne, Daniel J Rigden, Carl J Yung, Jessica Lingley, Michael A Quail, Neil Hall, Alistair C Darby, and Ilik J Saccheri. 2016. "The Industrial Melanism Mutation in British Peppered Moths Is a Transposable Element." *Nature* 534 (7605): 102–5.

Kobayashi, Yutaka, Peter Hammerstein, and Arndt Telschow. 2008. "The Neutral Effective Migration Rate in a Mainland-Island Context." *Theoretical Population Biology* 74 (1): 84–92.

Laetsch, Dominik R, Gertjan Bisschop, Simon Henry Martin, Simon Aeschbacher, Derek

Setter, and Konrad Lohse. 2022. "Demographically Explicit Scans for Barriers to Gene Flow Using gIMble." *bioRxiv*, 2022–10.

Manna, Federico, Guillaume Martin, and Thomas Lenormand. 2011. "Fitness Landscapes: An Alternative Theory for the Dominance of Mutation." *Genetics* 189 (3): 923–37.

Nagylaki, Thomas. 1975. "Conditions for the Existence of Clines." *Genetics* 80 (3): 595–615.

Nosil, Patrik. 2012. *Ecological Speciation*. Oxford University Press.

Otto, Sarah P. 1994. "The Role of Deleterious and Beneficial Mutations in the Evolution of Ploidy Levels." *Lectures on Mathematics in the Life Sciences* 25: 69–96.

———. 2003. "The Advantages of Segregation and the Evolution of Sex." *Genetics* 164 (3): 1099–1118.

Petry, Doug. 1983. "The Effect on Neutral Gene Flow of Selection at a Linked Locus." *Theoretical Population Biology* 23 (3): 300–313.

Sachdeva, Himani. 2022. "Reproductive Isolation via Polygenic Local Adaptation in Sub-Divided Populations: Effect of Linkage Disequilibria and Drift." *PLoS Genetics* 18 (9): e1010297.

Scott, Michael F, and Marie Rescan. 2017. "Evolution of Haploid–Diploid Life Cycles When Haploid and Diploid Fitnesses Are Not Equal." *Evolution* 71 (2): 215–26.

Scudo, Francesco M. 1967. "Selection on Both Haplo and Diplophase." *Genetics* 56 (4): 693.

Stankowski, Sean, Madeline A Chase, Hanna McIntosh, and Matthew A Streisfeld. 2022. "Integrating Top-down and Bottom-up Approaches to Understand the Genetic Architecture of Speciation Across a Monkeyflower Hybrid Zone." *Molecular Ecology*.

Westram, Anja M, Marina Rafajlović, Pragya Chaube, Rui Faria, Tomas Larsson, Marina Panova, Mark Ravinet, et al. 2018. "Clines on the Seashore: The Genomic Architecture Underlying Rapid Divergence in the Face of Gene Flow." *Evolution Letters* 2 (4): 297–309.

Westram, Anja M, Sean Stankowski, Parvathy Surendranadh, and Nick Barton. 2022. "What Is Reproductive Isolation?" *Journal of Evolutionary Biology* 35 (9): 1143–64.

Wright, Sewall. 1937. "The Distribution of Gene Frequencies in Populations." *Proceedings of the National Academy of Sciences* 23 (6): 307–20.

Yeaman, Sam. 2015. "Local Adaptation by Alleles of Small Effect." *The American Naturalist* 186 (S1): S74–89.

S1 Supplementary figures

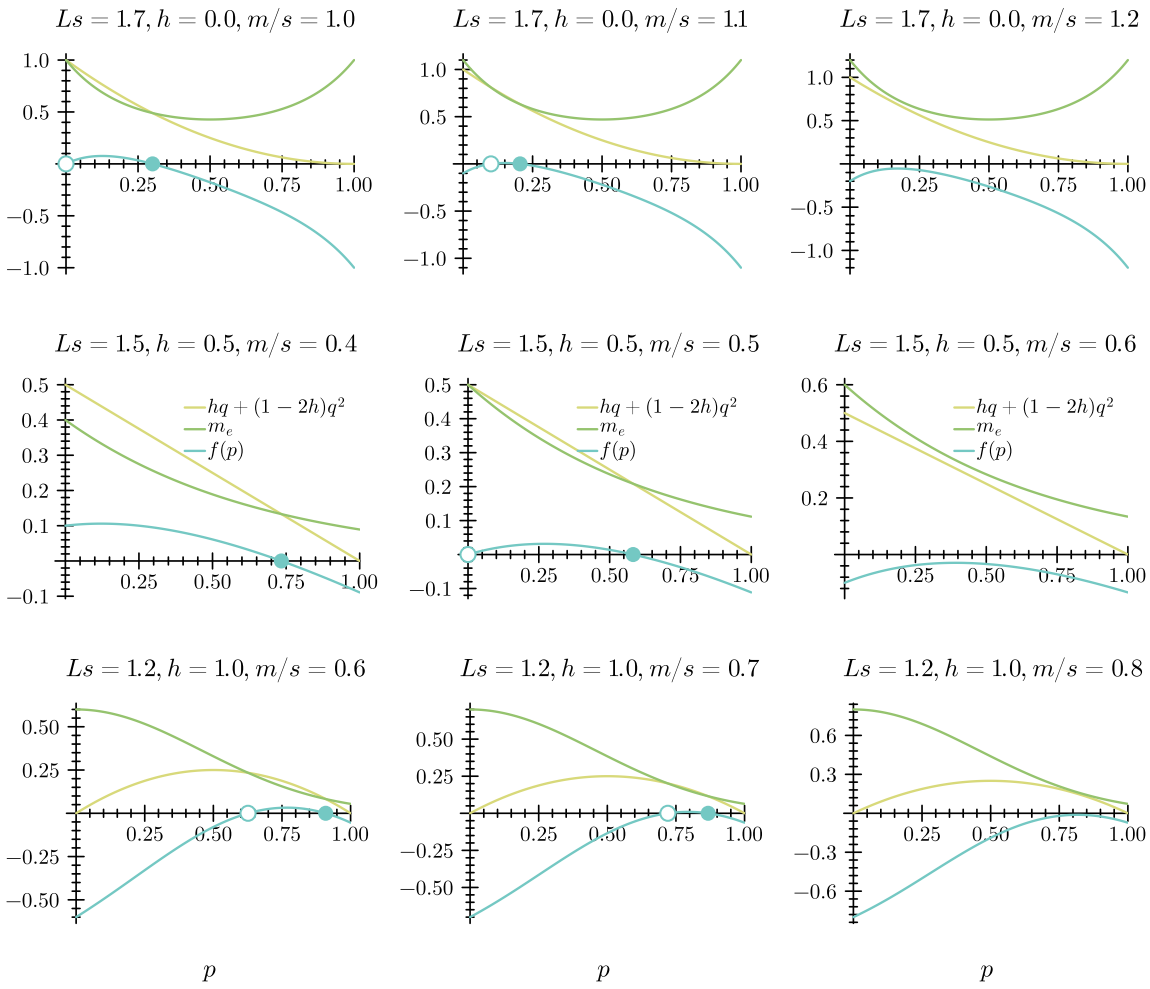

Figure S1: Critical swamping thresholds for the multilocus model. Equilibria of the multilocus system correspond to the zeros of $f(p) = hq + (1 - 2h)q^2 - m_e/s$. Examples for $f(p)$ in the case with dominant local adaptation (top row), additive local adaptation (middle row) and recessive local adaptation (bottom row) near the critical point. The stable equilibrium is indicated by a filled dot, the unstable by an unfilled dot. When there is bistability, i.e. both a stable and unstable equilibrium, the critical migration rate at which the two equilibria collide and cease to exist corresponds to the value of m for which $f(p)$ reaches its maximum in the critical point, so that both $f(p) = 0$ and $f'(p) = 0$ are satisfied.

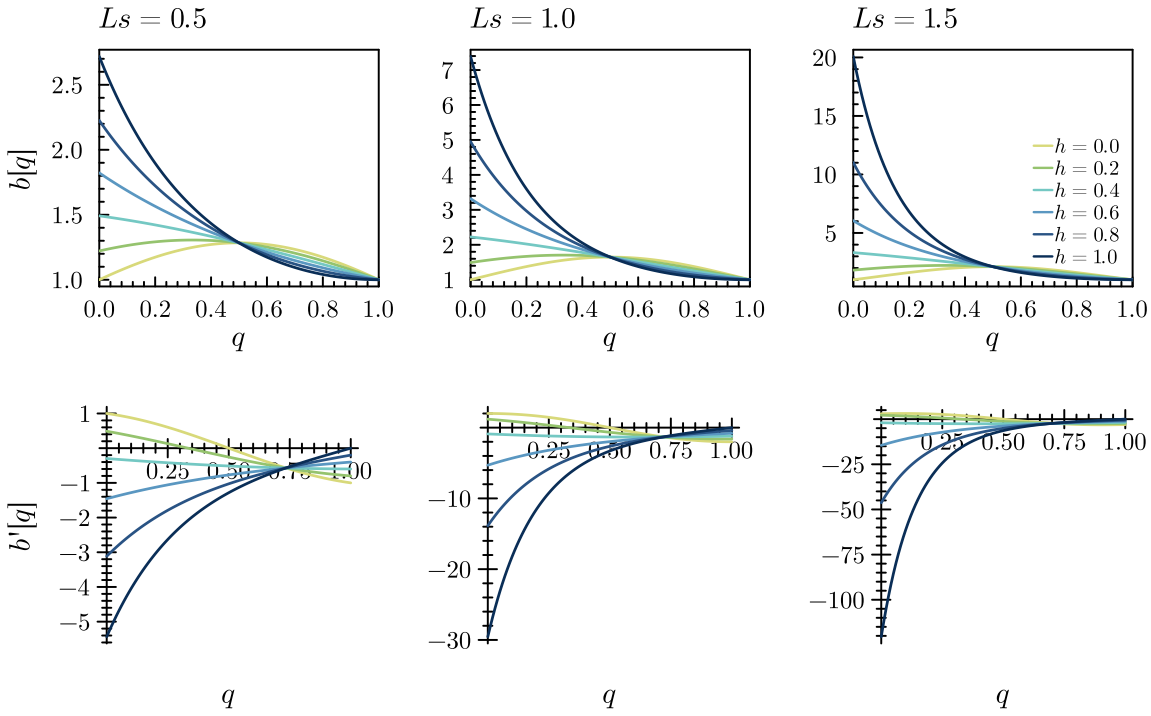

Figure S2: The barrier strength $b = g^{-1}$ (top row), and its derivative with respect to the deleterious allele frequency q (bottom row), for $Ls = 0.5, 1, 1.5$ (columns) and different degrees of (effective) dominance (h, colors).

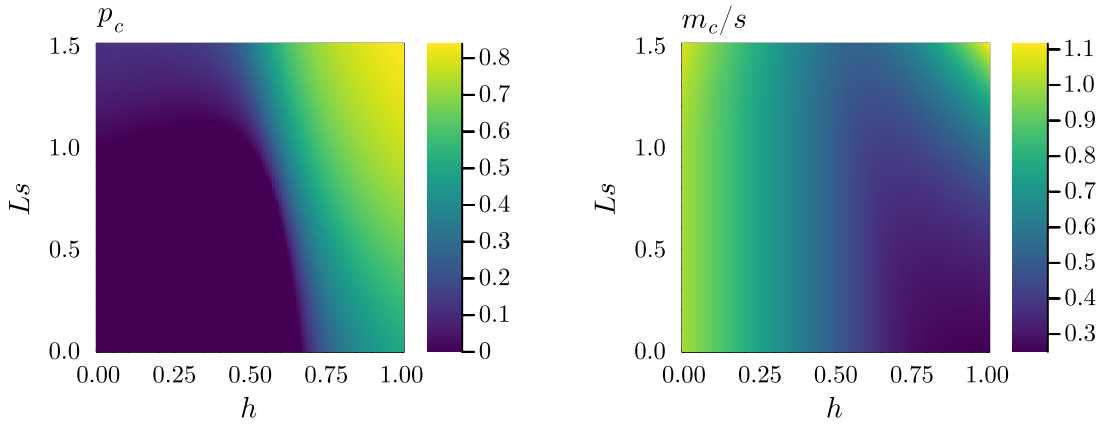

Figure S3: Critical equilibrium differentiation (p_c, the frequency of the locally beneficial allele on the island just before swamping) and critical migration rate (m_c) for intermediate dominance ($0 \leq h \leq 1$) and low to appreciable divergence ($Ls \leq 1.5$).

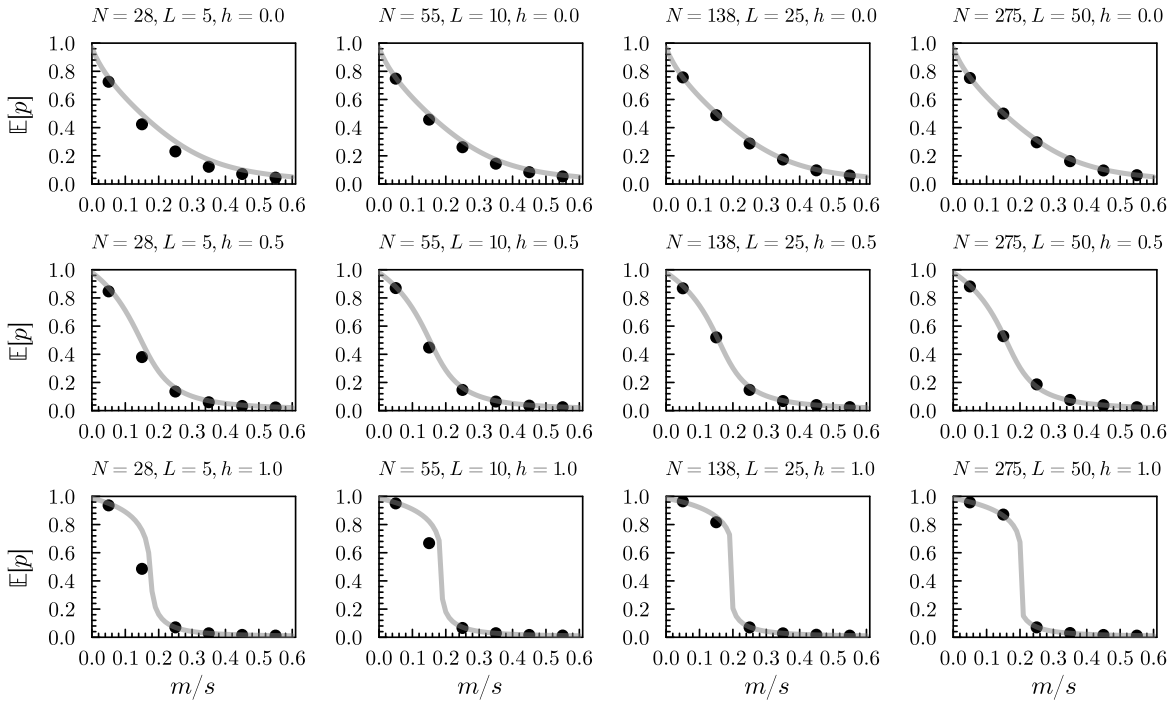

Figure S4: Comparison of the multilocus diffusion approximation (gray line) against individual-based simulations (black dots). $Ls = 1$ and $N_e s = 5$ for all plots, while L is varied across columns ($L \in [5, 10, 25, 50]$) and h varies over rows ($h \in [0, 0.5, 1]$). We assumed $k = 5$ diploids per haploid individual and set $N = N_e/2k + N_e$ so that the desired $N_e = N_e s/(Ls/L)$ is obtained. Allele frequencies for the individual-based simulations are obtained by simulating for 110000 generations, sampling every 5 generations after discarding the first 60000, and averaging across loci. For each L we simulate n replicates so that $nL = 50$. The mutation rate was set to $u = 0.005s$.

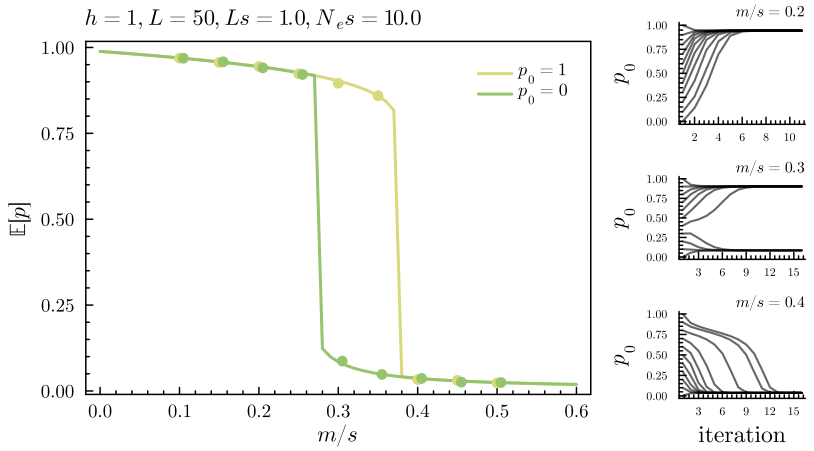

Figure S5: Different apparent equilibria depending on initial conditions. In the left plot, the yellow line ($p_0 = 1$) indicates the expected allele frequencies as determined using the fixed point iteration of algorithm S1, starting with $p^{(0)} = (1, 1, \ldots, 1)$ (i.e. secondary contact, maximal initial differentiation), whereas the green line assumes $p^{(0)} = (0, 0, \ldots, 0)$ (no initial differentiation). The dots show results from individual-based simulations with the same initial conditions (50000 generation, keeping the last 25000 and subsampling every 5 generations). The three plots on the right show the evolution of the fixed point iteration for different initial initial conditions $p^{(0)} = (p_0, p_0, \ldots, p_0)$ for three values of m. Note the bifurcation of the dynamical system defined by the algorithm: for $m/s = 0.2$ and $m/s = 0.4$ there is a single globally stable fixed point, whereas for $m/s = 0.3$, there are two locally stable fixed points.

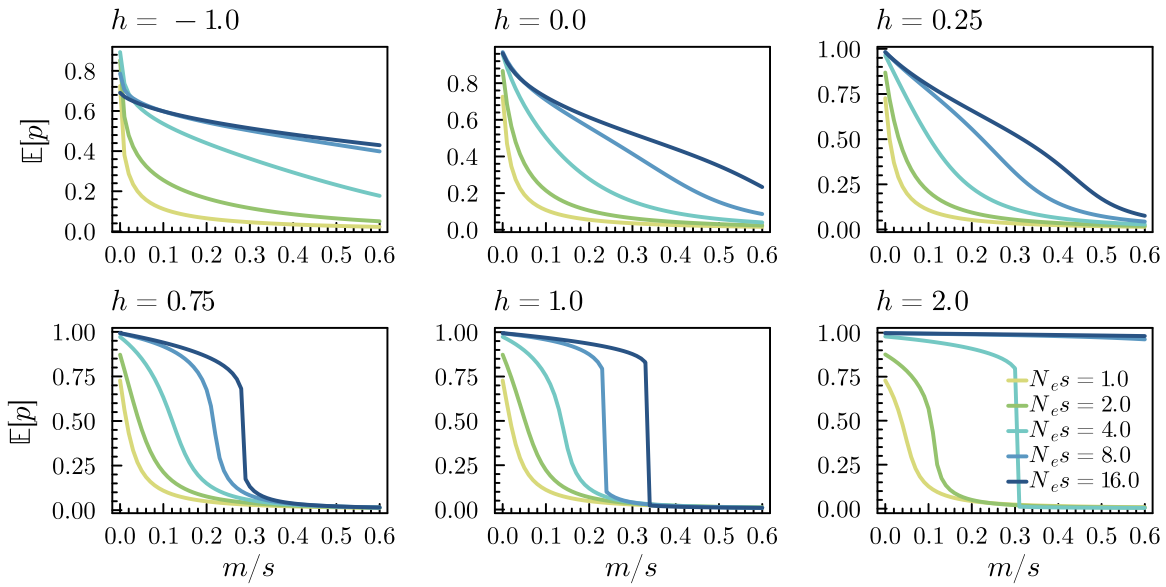

Figure S6: Effect of drift on equilibrium differentiation and swamping thresholds. All results use $L = 40, Ls = 0.8, k = 5$.

S2 Appendix

S2.1 Single locus allele frequency dynamics for weak selection

Consider a single locus in a population of organisms with a haplodiplontic life cycle. We assume a finite number n of alleles exist at the locus. Let p_i, $i \in [0..n-1]$, denote the frequency of the ith allele (A_i). Ignoring mutation and migration for now, the change in allele frequency of an allele A_i througout the life cycle is assumed to take the form:

$$\underbrace{p_i \underset{\text{haploid selection}}{\longrightarrow} p_i^* \underset{\text{gametogenesis}}{\longrightarrow} p_i^*}_{\text{haploid (gametophytic) phase}} \underset{\text{syngamy}}{\longrightarrow} \underbrace{p_i^* \underset{\text{diploid selection}}{\longrightarrow} p_i' \underset{\text{meiosis}}{\longrightarrow} p_i'}_{\text{diploid (sporophytic) phase}}, \tag{1}$$

where we have assumed that gametogenesis, syngamy and spore formation do not affect the allele frequencies. Generally, migration could take place at any stage in the life cycle, for instance right after meiosis (e.g. dispersal of meiospores in bryophytes and Fungi), at the end of the haploid phase (e.g. gamete dispersal in algae), early in the diploid phase (e.g. seed dispersal in spermatophytes) or at the level of adult diploids (e.g. migration in animals).

Let the relative haploid fitness of a haploid individual carrying allele i be $1+\epsilon s_i$, defined as the relative contribution to the diploid (sporophytic) generation within the haploid (gametophytic) generation. Similarly, we let $1 + \epsilon s_{ij}$ denote the relative fitness of a diploid individual with genotype A_iA_j. The allele frequency change over a single generation is determined by the following dynamical system:

$$\begin{aligned} p_i^* &= \frac{w_{g,i}}{\bar{w}_g(p)} p_i \\ p_i' &= \frac{w_{s,i}(p^*)}{\bar{w}_s(p^*)} p_i^* \qquad 1 \leq i \leq n, \end{aligned} \tag{2}$$

where $p = (p_1, p_2, \ldots, p_n)$ (and similarly for p^*). The marginal fitnesses $w_{g,i}$ and $w_{s,i}$ associated with allele A_i in the gametophytic and sporophytic phase respectively are

$$\begin{aligned} w_{g,i} &= 1 + \epsilon s_i \\ w_{s,i}(p) &= \sum_j (1 + \epsilon s_{ij}) p_j = 1 + \epsilon \sum_j s_{ij} p_j := 1 + \epsilon \bar{s}_{s,i}. \end{aligned}$$

The mean fitnesses in the gametophytic and sporophytic phases are

$$\begin{aligned} \bar{w}_g(p) &= \sum_i (1 + \epsilon s_i) p_i := 1 + \epsilon \bar{s}_g \\ \bar{w}_s(p) &= \sum_i \sum_j (1 + \epsilon s_{ij}) p_i p_j := 1 + \epsilon \bar{s_s} \end{aligned}$$

The allele frequency change over a single alternation of generations for the dynamical system defined in eq. 2 has the usual form

$$\Delta p_i = \frac{\bar{w}_i - \bar{w}}{\bar{w}} p_i \tag{3}$$

Where, from eq. 2, we have

$$\bar{w} = \Big(1 + \epsilon \sum_j \sum_k \frac{(1+\epsilon s_j) p_j (1+\epsilon s_k) p_k}{(1+\epsilon \bar{s}_g)^2} s_{jk}\Big)(1+\epsilon \bar{s}_g) = 1 + \epsilon \bar{s}_g + \frac{\epsilon \bar{s}_s}{(1+\epsilon \bar{s}_g)^2} + O(\epsilon^2) \quad (4)$$

and

$$\bar{w}_i = \Big(1 + \epsilon \frac{\sum_j s_{ij}(1+\epsilon s_j) p_j}{1 + \epsilon \sum_k s_k p_k}\Big)(1+\epsilon s_i) = 1 + \epsilon s_i + \frac{\epsilon \bar{s}_{s,i}}{(1+\epsilon \bar{s}_g)} + O(\epsilon^2),$$

so that

$$\bar{w}_i - \bar{w} = \epsilon(s_i - \bar{s}_g) + \frac{\epsilon}{(1+\epsilon \bar{s}_g)^2}(\bar{s}_{s,i} - \bar{s}_s) + O(\epsilon^2). \quad (5)$$

Assuming the intensity of selection per generation is weak (all s are small) and that ϵ measures the generation time, we obtain a continuous-time model of allele frequency change by considering the per-generation change in allele frequency and taking the limit as ϵ goes to zero, specifically, plugging eq. 5 and eq. 4 in eq. 3, we get

$$\begin{aligned} \dot{p}_i = \lim_{\epsilon \to 0} \frac{\Delta p_i}{\epsilon} &= \big[(s_i - \bar{s}_g) + (\bar{s}_{s,i} - \bar{s}_s)\big] p_i \\ &= (\bar{s}_i - \bar{s}) p_i, \end{aligned} \quad (6)$$

where

$$\begin{aligned} \bar{s}_i &= s_i + \bar{s}_{s,i} = s_i + \sum_j s_{ij} p_j \\ \bar{s} &= \bar{s}_g + \bar{s}_s = \sum_i s_i p_i + \sum_i \sum_j s_{ij} p_i p_j. \end{aligned} \quad (7)$$

This has the same form as the classical diploid or haploid continuous-time model of allele frequency change[2] but with marginal and mean Malthusian fitnesses given by $\bar{s}_i$ and $\bar{s}$ respectively.

As an example, consider the biallelic case with alleles A_0 and A_1, so that $s_0 = s_{00} = 0$, $p_0 = p$ and $p_1 = q$. Note that we shall always assume $s_{ij} = s_{ji}$. We have from eq. 7 $\bar{s}_1 = s_1 + s_{01} p + s_{11} q$ and $\bar{s} = s_1 q + 2 s_{01} pq + s_{11} q^2$. Some algebra shows that we can write the ODE for the frequency of the selected allele (A_1) as

$$\dot{q} = (\bar{s}_1 - \bar{s}) q = pq(r_1 + r_2 q) \quad (8)$$

where $r_1 = s_1 + s_{01}$ and $r_2 = s_{11} - 2 s_{01}$. As expected, this is the same dynamical law as for the strictly diploid model, in which case the dynamics of the selected allele are given by eq. 8 but with $r_1 = s_{01}$. This enables us to identify a pair of 'effective' selection coefficients,

$$\begin{aligned} s^*_{01} &= s_1 + s_{01} \\ s^*_{11} &= 2 s_1 + s_{11}, \end{aligned} \quad (9)$$

so that, for weak selection, a diploid biallelic model with parameters s^*_{01} and s^*_{11} yields the same allele frequency dynamics[3] as a haplodiplontic model with parameters s_1, s_{01} and s_{11}.

[2]The same result can be obtained in a slightly less cumbersome manner by first noting that, under the assumption of weak selection, allele frequency changes within a single alternation of generations are negligible, so that $w_{s,i}(p^*) = w_{s,i}(p)$ and $\bar{w}_s(p^*) = \bar{w}_s(p)$ in eq. 2.

[3]Note that a diploid model with these effective parameters does *not* yield the same mean fitness (and hence genetic load) as a haplodiplontic model in the original parameterization if we define mean fitness in the continuous time model as $\sum_i e^{s_i} p_i \big(\sum_j e^{s_{ij}} p_j\big)$.

S2.2 Equilibrium structure of the mainland-island model

We describe the equilibrium structure of the haplodiplontic single-locus deterministic mainland-island model for the biallelic case. The dynamics are given by the ODE

$$\dot{q} = -\dot{p} = m\Delta q + pq(s_a + s_b q) \tag{10}$$

$$= m\Delta q + pq(s_1 + s_{01} + (s_{11} - 2s_{01})q), \tag{11}$$

where q is the frequency of the locally selected allele A_1, and $p = 1 - q$ is the frequency of the allele with relative fitness of 1 on the island when homozygous.

When $m = 0$ (no migration), there will be an admissible fixed point when either of the following conditions holds

$$s_{01} > -s_1 \text{ and } s_{01} > s_1 + s_{11} \tag{12}$$

$$s_{01} < -s_1 \text{ and } s_{01} < s_1 + s_{11}, \tag{13}$$

i.e. when there is *ploidally antagonistic selection*. The fixed point is obtained at

$$\tilde{p} = \frac{s_a + s_b}{s_a} = \frac{s_1 + s_{11} - s_{01}}{s_{11} - 2s_{01}} \tag{14}$$

This will correspond to a stable polymorphism whenever $s_{01} > 0$. This case was first analyzed in a discrete-time model by Scudo (1967).

Now consider $m > 0$. We shall assume that $\Delta q = q_{\text{mainland}} - q = 1 - q = p$, i.e. the mainland is fixed for the locally selected allele. To describe the equilibrium behavior, it is helpful to factor the dynamical law as

$$\dot{q} = mp\left(1 + \frac{s_a}{m}q + \frac{s_b}{m}q^2\right) \tag{15}$$

Linear stability at a fixed point $\tilde{q}$ is determined by

$$\frac{d\dot{q}}{dq}\Big|_{\tilde{q}} = (s_a - m) + 2(s_b - s_a)\tilde{q} - 3s_b\tilde{q}^2 \tag{16}$$

If $s_b = 0$, we have an effectively haploid model (i.e. *genic selection*), and will have a stable polymorphic equilibrium at $\tilde{q} = -m/s_a$ whenever $m < -s_a$, and a stable boundary equilibrium at $\tilde{q} = 1$ when $m > -s_a$. When $s_b \neq 0$, polymorphic equilibria, when they exist, will correspond to the roots of the quadratic expression in parentheses in eq. 15. These are

$$q_-, q_+ = \frac{-s_a/m \pm \sqrt{(s_a/m)^2 - 4s_b/m}}{2s_b/m}$$

We have the following biologically relevant equilibria:

i. $\tilde{q} = 1$ (*swamping*) is always a stable equilibrium when $m > -(s_a + s_b)$.
ii. When $0 < m < -(s_a + s_b)$ there is always a single stable polymorphic equilibrium at q_- (dark gray zone in fig. S7) and q_+ will not lie in $[0, 1]$.
iii. When $-(s_a + s_b) < m < s_b$ and $4s_b/m < (s_a/m)^2 \iff 4m < s_a^2/s_b$, there is, besides the stable boundary equilibrium at $\tilde{q} = 1$, an unstable (repelling) equilibrium at q_+, and a stable polymorphic equilibrium at q_- (light gray zone in fig. S7).

The relation between the key parameters s_a/m and s_b/m and the equilibrium behavior of the system when $m > 0$ is illustrated in fig. S7.

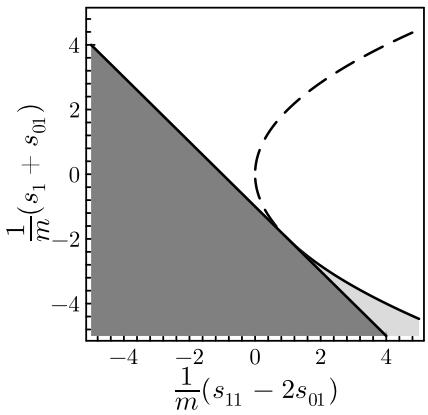

Figure S7: Equilibrium and stability behavior of the single-locus biallelic haplodiplontic mainland-island model. The dark gray zone indicates the parameter region where there is a single protected stable polymorphic equilibrium. The light gray zone shows the parameter region where there is both a stable (but unprotected) and an unstable polymorphic equilibrium. s_1, s_{01} and s_{11} are the haploid and diploid selection coefficients for the invading allele (A_1) on the island.

S2.3 Two-locus haplodiplontic mainland-island model

We here consider the deterministic dynamics of a two-locus haplodiplontic model with mainland-island migration in continuous-time. We assume a locus A with alleles A_0 and A_1 and a linked locus B with alleles B_0 and B_1, with recombination between the two loci occurring at rate r. We assume arbitrary dominance and no epistasis, with relative Malthusian fitnesses of all possible two-locus genotypes in the two phases given by the following tables

Haploid

	B_0	B_1
A_0	0	β_1
A_1	α_1	$\alpha_1 + \beta_1$

Diploid

	B_0B_0	B_0B_1	B_1B_1
A_0A_0	0	β_{01}	β_{11}
A_0A_1	α_{01}	$\alpha_{01} + \beta_{01}$	$\alpha_{01} + \beta_{11}$
A_0A_1	α_{11}	$\alpha_{11} + \beta_{01}$	$\alpha_{11} + \beta_{11}$

(17)

Similar to our notation for the single-locus case, we let $\alpha_a = \alpha_1 + \alpha_{01}$ and $\alpha_b = \alpha_{11} - 2\alpha_{01}$ (and similarly for β_a and β_b). Let x_{ij} and y_{ij} denote the frequency of the A_iB_j haplotype on the island and mainland respectively. The two-locus dynamics in continuous-time are given by

$$\dot{x}_{ij} = m(y_{ij} - x_{ij}) + (\omega_{ij} - \bar{\omega})x_{ij} - \eta_{ij} r D \tag{18}$$

where $D = x_{00}x_{11} - x_{01}x_{10}$ is the usual measure of linkage disequilibrium, ω_{ij} the marginal fitness of the A_iB_j haplotype, $\bar{\omega}$ the mean Malthusian fitness and $\eta_{ij} = 1$ when $i = j$ and -1 otherwise. Defining

$$Q_A = \alpha_a + \alpha_b q_A \qquad Q_B = \beta_a + \beta_b q_B$$
$$P_A = \alpha_a + \alpha_b p_A \qquad P_B = \beta_a + \beta_b p_B,$$

one can find that $\bar{\omega} = q_A Q_A + q_B Q_B$ and write the marginal fitnesses as

$$\begin{aligned}
\omega_{00} - \bar{\omega} &= -q_A Q_A - q_B Q_B \\
\omega_{01} - \bar{\omega} &= \beta_a - q_A Q_A - q_B P_B \\
\omega_{10} - \bar{\omega} &= \alpha_a - q_A P_A - q_B Q_B \\
\omega_{11} - \bar{\omega} &= \alpha_a + \beta_a - q_A P_A - q_B P_B.
\end{aligned} \tag{19}$$

Let $p_A = x_{00} + x_{01}$ be the allele frequency of A_0 and $p_B = x_{00} + x_{10}$ that of B_0, and let $q_A = 1 - p_A$ and $q_B = 1 - p_B$. We shall assume that the mainland is fixed for haplotype A_1B_1 (i.e. $y_{11} = 1$). Using eq. 19 with eq. 18, one can derive the dynamics for p_A, p_B and D:

$$\begin{aligned}
\dot{p}_A &= -m p_A - p_A q_A Q_A - Q_B D \\
\dot{p}_B &= -m p_B - p_B q_B Q_B - Q_A D \\
\dot{D} &= m(p_A p_B - D) + (Q_A(p_A - q_A) + Q_B(p_B - q_B))D - rD.
\end{aligned} \tag{20}$$

We can use eq. 20 to derive the effective migration rate at a neutral locus linked to a barrier locus maintained at migration-selection balance. Let A be the selected locus, and B the linked neutral locus. The dynamics of the system are given by eq. 20, where $Q_B = 0$. Assuming r is sufficiently large (linkage is sufficiently weak) so that D equilibrates much faster than the allele frequencies, we can solve the system for D at equilibrium to find

$$\tilde{D} = \frac{m p_A p_B}{m + r - Q_A(p_A - q_A)} \tag{21}$$

We can plug this into the ODE for the neutral locus to find

$$\dot{p}_B = -m \left(1 + \frac{p_A Q_A}{m + r - Q_A(p_A - q_A)}\right) p_B \tag{22}$$

Suggesting that the effective migration rate under the stated assumptions should be

$$m_e = m \left(1 + \frac{p_A Q_A}{m + r - Q_A(p_A - q_A)}\right) \approx m \left(1 + \frac{p_A Q_A}{r}\right), \tag{23}$$

where the approximation holds well for weak linkage, which we assumed when we derived eq. 22.

S2.4 Fixed point iteration algorithm

Our approximations yield a system of equations for the expected allele frequencies and heterozygosities on the island which are coupled through the gff. To calculate expected allele frequencies and allele frequency distributions at equilibrium, we solve the system self-consistently by performing a fixed point iteration. In words: for a given initial set of allele frequencies and heterozygosities, we calculate the gff at each locus using eq. 9; using these gff values, we next calculate expected allele frequencies and heterozygosities at each locus using numerical quadrature. This process is repeated until convergence. The algorithm is more formally outlined in algorithm S1.

Algorithm S1 Fixed point iteration for calculating the expected allele frequency and expected heterozygosity on the island.

Require: Initialization $p^{(0)} = (p_1^{(0)}, \ldots, p_L^{(0)})$, tolerance ϵ

$(pq)^{(0)} \leftarrow (p_1^{(0)} q_1^{(0)}, \ldots, p_L^{(0)} q_L^{(0)})$

$n \leftarrow 1, \Delta \leftarrow \infty$

while $\Delta > \epsilon$ **do**

  for $j = 1, \ldots, L$ **do**

    $m_{e,j}^{(n)} \leftarrow \exp\left[\sum_{i \neq j} s_{a,i} q_i^{(n-1)} + s_{b,i} (p_i q_i)^{(n-1)}\right]$

    $p_j^{(n)} \leftarrow \int_0^1 p \phi(p; N_e, u, m_{e,j}^{(n)}, s_j) dp$

    $(p_j q_j)^{(n)} \leftarrow \int_0^1 p(1-p) \phi(p; N_e, u, m_{e,j}^{(n)}, s_j) dp$

  end for

  $\Delta \leftarrow \sum_j (p_j^{(n)} - p_j^{(n-1)})^2$

  $n \leftarrow n + 1$

end while

return $p^{(n)}, (pq)^{(n)}$